Study on the failure probability of a rock slope in consideration of the uncertainty of mechanical and hydraulic properties

Akash Chakraborty [(1)] ***Kuang-Tsung Chang*** [(2)]

Graduate Student [(1)], Professor [(2)] in the Department of Soil and Water Conservation, National Chung Hsing University, Taiwan

ABSTRACT

Typhoons and extreme rainfall conditions typically lead to failure and collapse in rock slopes with steep geological features. The Lushan slope, located in the central region of Taiwan, has been undergoing sliding due to similar rainfall conditions over the past decades. In regular slope stability analyses, the average values of strength parameters are used to estimate the factor of safety (FS). However, natural slope materials often exhibit significant variability, making it challenging to assess slope stability based solely on fixed parameter values. Due to this inherent uncertainty in geotechnical properties, evaluating the probability of slope failure has become essential for a more realistic and reliable assessment of slope stability. In this study, the uncertainty of mechanical and hydraulic parameters is considered to explore the probability of failure in rock slopes, which can be used as a reference for the risk assessment and early warning systems of large-scale collapse. Stochastic Finite Element Method (SFEM) analysis was conducted through the Monte Carlo Simulation (MCS) method to perform random sampling and generate combinations of parameters as random variables with uncertainty. The results show that the probability of failure of the Lushan slope with rainfall duration of 2 days and return intervals of 100 and 500 years ranges from 22 to 27 %, while for the rainfall duration of 3 days and return intervals of 100 and 500 years it ranges from 30 to 35 %.

(**Keywords:** Lushan slope, unsaturated hydraulics, parameter uncertainty, probability of failure)

[(1)]PhD student, National Chung Hsing University

[(2)]Professor, National Chung Hsing University (Corresponding author e-mail：changkt@nchu.edu.tw)

Introduction

Deep-seated landslides in rock slopes are common in steep terrain under intense rainfall. Because slope stability assessments are affected by uncertainty in topography, geology, and model parameters, reliability analysis is widely used to quantify how parameter uncertainty influences failure risk (Morgenstern, 1997). In regular slope stability analyses, the average values of strength parameters are used to estimate the factor of safety (FOS). However, natural slope materials often exhibit significant variability, making it challenging to assess slope stability based solely on fixed parameter values. The material state of the slope changes with space or time, such as soil or rock properties, weak surface conditions, etc. The geological conditions and analysis parameters of natural slopes are difficult to grasp, causing uncertainties and affecting the slope stability results. Considering these uncertainties, analyzing the collapse probability can provide a more objective assessment of the slope's stability. Consequently, engineering practice typically couples limit equilibrium or finite element analyses with approximate reliability methods (e.g., point estimate, first-order second-moment, FORM) or Monte Carlo simulation (Malkawi et al., 2000; Hammah & Yacoub, 2009). When finite elements are combined with Monte Carlo simulation, the approach is referred to as the stochastic finite element method (SFEM). Comparative studies indicate that point estimate methods can be accurate for low-dimensional problems but may lose accuracy as dimensionality increases, whereas Monte Carlo simulation remains a direct and practical option given modern computational resources (Hammah & Yacoub, 2009). In this study, the uncertainty of mechanical and hydraulic parameters along with different rainfall designs is considered to explore the probability of failure, which can be used as a reference for the risk assessment and warning systems of large-scale landslides.

Research methods

1. Study area

The Lushan slope, located in the central region of Taiwan, has been undergoing sliding due to extreme rainfall conditions over the past decades (Figure 1). The Lushan Slope is the northern slope of Lushan Hot Spring and Taluowan Creek in Renai Township, Nantou County. The length and width of the sliding area are approximately 820 meters and 480 meters, respectively. The top of the sliding area is close to the triangular point of Muan Mountain, with an altitude of about 1,495 meters, and the toe is located near the river valley. The elevation difference between the upper and lower sides of the sliding body is about 410 meters, covering an area of about 30 hectares. The toe is located near the Taluowan stream valley.

Figure 1 Panoramic view of the Lushan landslide area (Modified form Chang and Huang, 2015)

The slope geometry and sliding surface in this study are based on Chang et al. (2015). The Lushan slope sliding surface was investigated with inclinometers to find a maximum sliding depth of about 100 meters (Figure 2). The Lushan Formation is the main slate formation in the Central Mountains. According to drilling data from the Soil and Water Conservation Bureau (2006), the formation here is mainly composed of interbedded black to dark gray argillite, slate, and dark gray hard sandstone. The model was divided into a sliding body (Hoek-Brown material) and a surrounding part (elastic material).

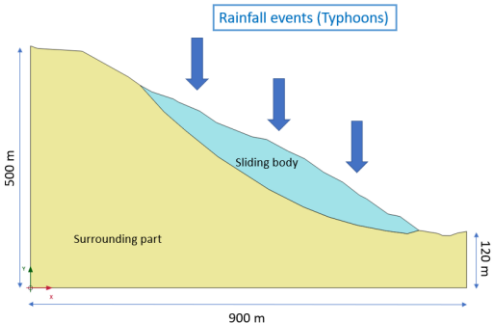

Figure 2 Model geometry in 2D

2. Van-Genuchten model

Rising groundwater levels have more impact on deep-seated landslides than shallow ones. Long-lasting rainfall usually causes a significant rise in groundwater levels. Groundwater level rise from rainfall depends on factors such as rainfall intensity and type, as well as unsaturated and saturated permeability. Unsaturated permeability increases with water content, while saturated groundwater flow is governed by the saturated permeability. After rainfall infiltrates the ground, the flow of unsaturated water between the surface and the groundwater table is generally defined by the Soil Water Characteristic Curve (SWCC). The most commonly used is the Van-Genuchten (VG) model (Van Genuchten, 1980), which is described in PLAXIS as follows (Brinkgreve et al., 2016):

$$S(\psi) = S_{res} + \frac{S_{sat} - S_{res}}{[1 + g_\alpha |\psi|^{g_n}]^{1-1/g_n}} \quad (1)$$

where S_{sat} is the saturation when the pores are filled with water (PLAXIS default is 1), S_{res} is the residual saturation, $|\psi|$is the pressure head, $g_\alpha$is related to the air entry value of the soil (g_α > 0, cm $^{-1}$), and g_n is a function of the rate of water extraction from the soil. These three parameters are entered in PLAXIS 2D to create the SWCC curves (Figure 3).

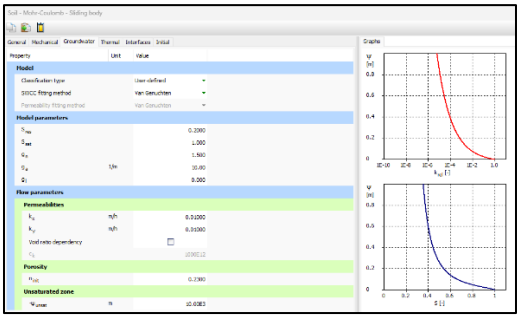

Figure 3 VG parameters & SWCC in PLAXIS 2D

3. Back-calculation of unsaturated parameters

In this study, the VG model was used to represent the unsaturated hydraulic behavior of the slope. The VG parameters g_a (air entry value), g_n, and g_l (fitting parameters) were used to match the groundwater level (GWL) conditions of the real slope. The g_l was fixed at zero. The GWL data of Typhoon Saola in 2012 and Typhoon Soulik in 2013 were collected from A21, A24, and A25 boreholes (Figure 4 a).

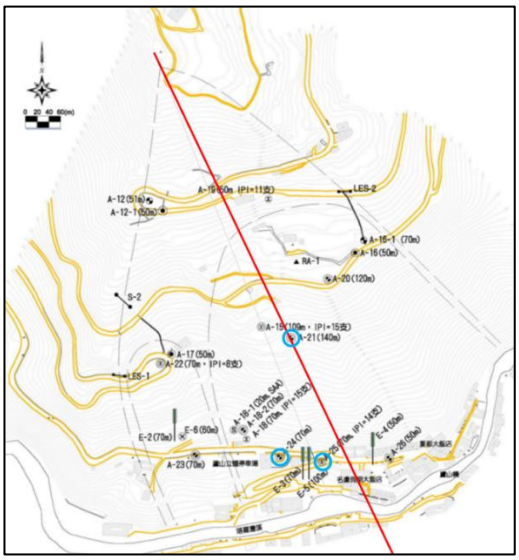

(a)

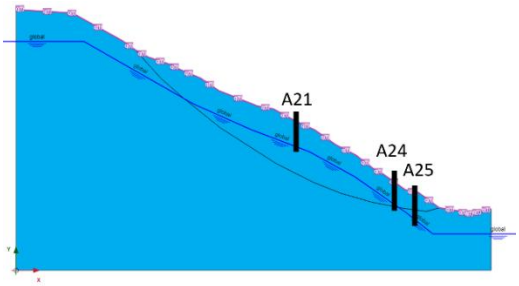

(b)

Figure 4 (a) Borehole locations (Central Geological Survey, 2012) (b) Groundwater settings

The initial groundwater level was created according to the collected borehole data, as shown in Figure 4 (b). The back calculation was done by matching the GWL rise of two rainfall events – Typhoon Saola and Soulik. Back-calculating unsaturated parameters from observed groundwater level rise in PLAXIS 2D is essential for accurately modeling rainfall–infiltration processes in real field conditions. It allows improving the reliability of slope stability and seepage analyses under transient conditions. The Root Mean Square Error (RMSE) method (Yang et al. 2019) was used to get the best fit and minimum errors (Figure 5). RMSE is a statistical metric that measures the average magnitude of errors between predicted and observed values, expressed in the same units as the data. It is calculated by taking the square root of the mean of squared differences between predictions and observations, which penalizes larger errors more heavily. A lower RMSE indicates better model performance, with zero representing a perfect fit. The RMSE values lay in the range of 0.7 to 1.56, which is acceptable and will not influence the transient analysis results. The RMSE equation is as follows:

$$RMSE = \sqrt{\frac{1}{n}\sum_{i=1}^{n}(M_i - S_i)^2} \quad (2)$$

where n is the total number of runs, M is the measured/monitored value, and S is the simulated/predicted value for each set.

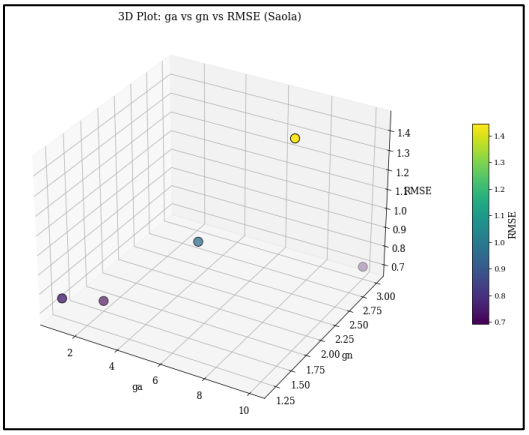

(a)

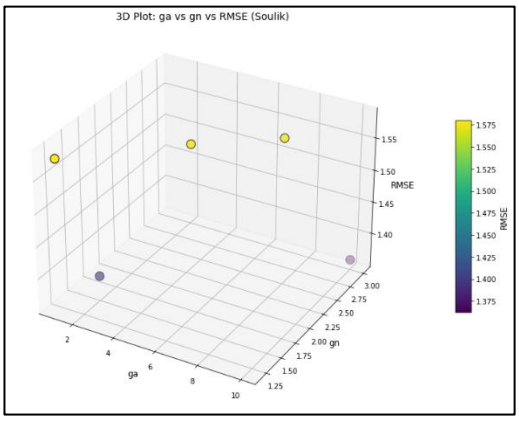

(b)

Figure 5 RMSE for back-calculated results from matching the (a) Saola and (b) Soulik typhoons

4. Determination of rock mass parameters

The Hoek-Brown model was used for the sliding body. The Hoek–Brown (HB) criterion is an empirical, non-linear strength model used to estimate the failure envelope of fractured rock masses by relating major and minor principal stresses; it bridges intact-rock laboratory strength with field geological conditions. Key inputs are m_i, the material constant, GSI (Geological Strength Index), a field-based index describing rock-mass structure and surface condition (jointing, block size, roughness) that controls degradation from intact to mass behavior; σ_{ci}, the uniaxial compressive strength of the intact rock; and D, the disturbance factor which quantifies the strength reduction of rock mass due to external factors like excavation damage, blasting, weathering, earthquakes, etc.

The mi was selected as 7, as the Lushan sliding area is dominated by slate. The GSI range was determined based on the rock core data available for the Lushan slope (Central Geological Survey, 2012) (Figure 6 (a)). The range was set as 20 to 40 after determining from the GSI scoring chart for cores proposed by Cai et al., 2007 (Figure 6 (b)). The block size was determined as blocky/disturbed (joint spacing 3 – 10 cm) and block condition as both fair and poor, as observed from the rock cores. The disturbance factor was back-calculated from matching stress curves of previous studies (Chang et al., 2015) as shown in Figure 7. It was computed as 0.83 and can be explained by earthquakes, weathering, etc., in natural slopes.

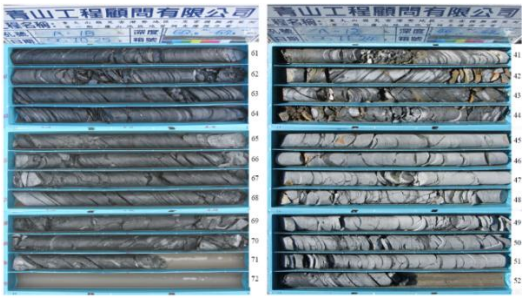

(a)

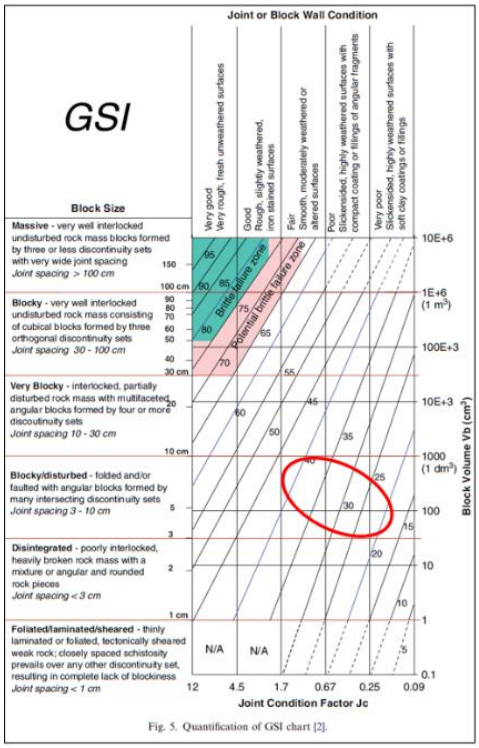

Fig. 5. Quantification of GSI chart [2].

(b)

Figure 6 (a) Rock cores from the slope (b) GSI range determination (modified from Cai et al., 2007)

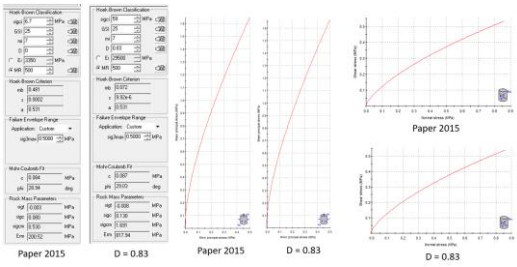

Figure 7 Matching stress curves to obtain the disturbance factor

All the mechanical parameters used for the two material types of the model are tabulated in Table 1. The unit weights and elastic parameters were obtained from Chang et al. (2015).

Table 1 Slope model parameters

Rock type	Slate	Sandy slate
Model part	Sliding body	Surrounding part
Material Model	Hoek- Brown	Linear Elastic
Unit weight (kN/m3)	26.2	26.2
Saturated unit weight (kN/m3)	26.4	26.4
Young's modulus (kN/m3)	2.00E+05	2.00E+06
Poisson's ratio	0.3	0.3
Intact uniaxial compressive strength (MPa)	59	
Material constant (mi)	7	
Disturbance factor (D)	0.8	
Permeability (m/h)	0.01	0.01

5. Rainfall design with variable return intervals and rainfall durations

The rainfall events are introduced in the model through the infiltration boundary on the surface of the slope. A synthetic rainfall event is labeled with a return period (10-, 50-, 100-year), a duration (12-hr, 24-hr, 48-hr), and a pattern (whether rain is advanced, peaked in the middle, delayed, spread out, etc.). The design rainfall depth is obtained from observed rainfall records by performing frequency analyses for a range of rainfall event durations to derive the intensity–duration–frequency (IDF) relationship. The IDF curve is then used to estimate the rainfall intensity with different rainfall durations and return periods. This result is then substituted into a time distribution function to obtain the temporal distribution of rainfall. This distribution function is called the design rainfall pattern.

In order to understand the impact of extreme rainfall events on the Lushan slope, a series of rainfall events was designed following the guidelines proposed by the Bureau of Water Resources (2001) (Figure 8). The pattern was a middle-peak distribution as described in the guidelines. These designs are then added to run the fully coupled transient rainfall analyses in the model of the Lushan slope.

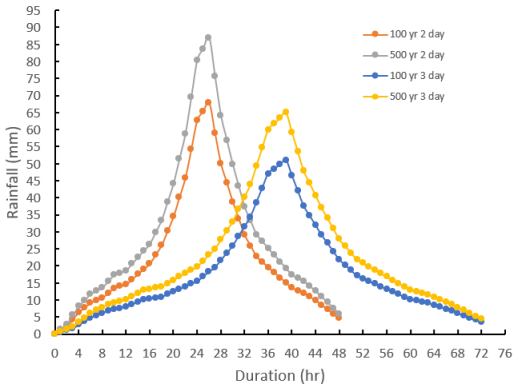

Figure 8 Rainfall designs for 2 return intervals & 2 rainfall durations

6. Multiple slope stability analyses using FEM automation program

An automated FEM slope-stability program runs large batches of analyses faster, hands-free, and consistently**,** replacing manual setup and clicking with scripted workflows. It auto-generates geometries/ meshes, assigns materials and groundwater conditions, executes and solves in parallel, and post-processes FOS, displacements, and failure modes into tables and plots. Parameter sweeps and Monte-Carlo runs become easier to perform, improving efficiency and reproducibility while eliminating transcription errors. This saves time, as manual handling can be time-consuming and hectic, especially when the number of runs exceeds 1000, 10000, or more.

In this study, the pyautogui and plxscripting modules in Python were implemented to automate the multiple slope stability analyses. Log files with different parameter sets were created, and then all the log files were put in a batch file (Figure 9). When a batch file is run, it auto-inputs the parameters from several log files and then autoruns all the transient slope stability analyses in PLAXIS 2D using computer commands. This method assists in doing many complex tasks automatically through command codes without manual touch (clicking buttons, opening and closing software, selecting options, typing parameters, etc.). The procedure for the whole research has been shown in Figure 10.

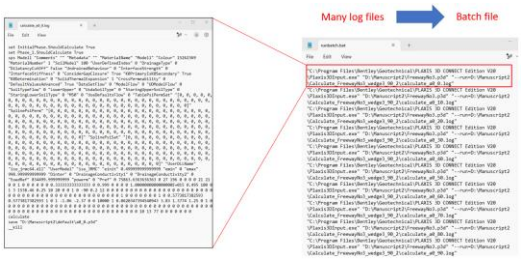

Figure 9 Log file & batch file for automatic slope stability analyses

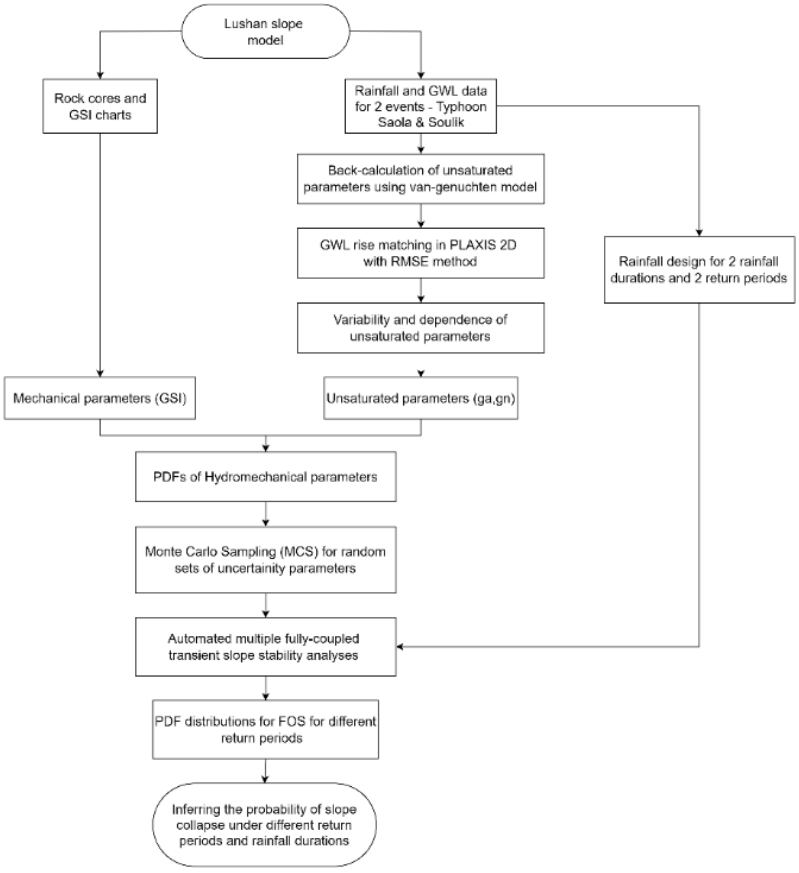

Figure 10 Whole procedure for this study

7. Monte Carlo simulation and sampling

In this study, the uncertainty of mechanical and hydraulic parameters is considered to explore the probability of failure in the Lushan slope using the Stochastic Finite Element Method (SFEM) analysis and Monte Carlo Simulations (MCS). However, Monte Carlo methods for probabilistic analysis of slope stability require multiple runs of calculations, and the more runs in the analysis, the more accurate the results. The SLOPE/W manual recommends the number of Monte Carlo experiments required (GEO-SLOPE International Ltd, 2012). This depends on the confidence interval required in the solution and the number of variables considered, and can be determined using the statistical formula:

$$N_{mc} = \left[\frac{d^2}{4(1-\varepsilon)^2}\right]^m \quad (3)$$

where N_{mc} is the number of Monte Carlo trials, ε is the confidence interval (0-100%), d is the normal standard deviation corresponding to the confidence interval, and m is the number of variables. For example, when the confidence interval is set to 80%, the corresponding normal

standard deviation can be found to be 1.28 using the normal distribution table. When the number of variables considered is 1, 2 or 3, the number of tests is 10, 100 or 1000 times, respectively. For more variables, the number of runs increases exponentially. In this study, as the number of variables is 3, 1000 runs were considered. The Monte Carlo sampling method from Excel was used to determine several parameter combinations (in our case GSI, ga, and gn) for FOS calculations with all rainfall designs (Figure 11).

Sl. No.	GSI	Ga	Gn
1	29.9415	7.43063	1.6837
2	25.6488	4.91857	1.41812
3	28.8453	6.78687	1.57826
4	30.9844	4.86854	2.13523
5	33.1464	4.38372	1.85804
6	35.9676	5.43705	1.89688
7	33.1607	3.66233	2.14949
8	31.6071	4.88146	1.98769
9	25.627	5.20881	1.569
10	26.6477	4.51623	2.08353
11	27.5688	3.46326	1.6869
I	I	I	I
I	I	I	I
I	I	I	I
996	28.2687	6.01479	1.85853
997	30.4359	4.23528	1.33206
998	29.6408	4.66072	1.6676
999	30.7651	6.00161	2.35674
1000	32.8371	6.31975	2.19537

Figure 11 Monte Carlo random sampling in Excel

Results and discussion

1. Variability and dependence of uncertainty parameters

In reliability and risk analysis, variability (the spread of each input) and dependence (how inputs co-vary) jointly determine outcomes to avoid biased probabilities of failure. Underestimating variability shrinks tails and hides extremes, while ignoring dependence or correlation can severely miscalculate failure, especially when critical variables rise together. In this study, the slope collapse probability analysis first explored the variability and dependence between unsaturated parameters, g_α, a value related to the inverse of air intake suction and g_n, a quantity related to the pore size distribution, before carrying out subsequent analysis. The coefficient of variation was calculated through the following equation,

$$\mathrm{COV}(x) = \frac{\sigma}{\mu} \tag{4}$$

where σ is the standard deviation of the parameter, μ is the mean value of the parameter, and the larger the COV, the greater the degree of variation. COV is a stable measurement of the degree of variation. When COV < 10%, it is a small degree of variation. When COV is between 15 and 30%, it is a medium degree of variation. When COV > 30%, it is a large degree of variation. The degree of variation for the 3 parameters was checked and found to be in the range of medium variations (10 ~ 30%) (Harr, 1987). The means, standard deviations, and COVs of the 3 parameters are listed in Table 2. For the unsaturated parameters, they were obtained from the back analysis results, while for the GSI, the three-sigma rule (Duncan, 2000) was used to calculate the standard deviation from their Highest Conceivable value (HCV) and Lowest Conceivable value (LCV) obtained through GSI charts.

$$\sigma = \frac{HCV - LCV}{6} \tag{5}$$

Table 2 Statistical parameters for probability distributions

Variables	GSI	ga	gn
Highest Predictable value (HCV)	40	From back calculated average	
Lowest Predictable value (LCV)	20		
Average/Mean (μ)	30	5.072	2.043
Standard deviation (σ)	3.333	1.382	0.338
Coefficient of variation (COV)	0.111	0.273	0.154
Coefficient of variation (COV) %	11.1	27.3	15.4

The dependence between the back-calculated unsaturated parameters was observed and calculated using the Pearson correlation coefficient (Benesty et al., 2009) and was found to be -0.14. The value is close to zero, which means the variables are almost uncorrelated and independent (Figure 12). The weak negative value suggests a tiny negative trend, but it is so weak that it could be due to random noise or nonlinear factors. The correlation between unsaturated parameters or parameter uncertainty has been explored in many studies (Johari and Talebi, 2019; Wang et al., 2020).

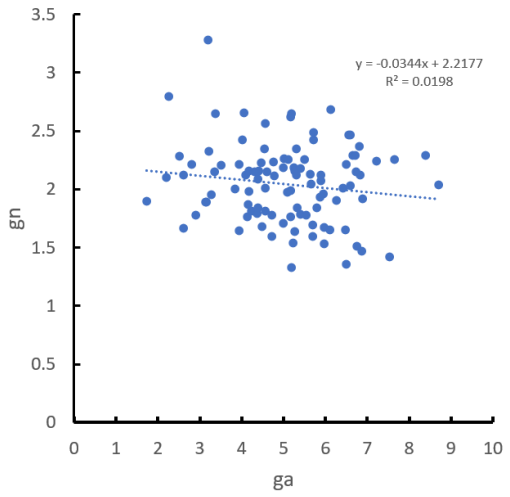

Figure 12 Dependence of unsaturated parameters

2. PDFs of hydromechanical parameters

A probability density function (PDF) describes how likely a continuous random variable is to take values across its range. PDFs summarize key features like center, spread, skew, and tails (which drive risk/extremes). Most PDFs follow normal, lognormal, or gamma distributions. The probability distributions of the three uncertainty parameters GSI, g_a, and g_n were drawn from their statistical parameters, and it was observed that they follow the normal distribution (Figure 13). The normal distribution is the most commonly used probability distribution in engineering, and its probability density function is defined as follows (Chow, 1988; Chowdhury, 2023):

$$f(x) = \frac{1}{\sigma\sqrt{2\pi}} \exp\left[-\frac{(x-\mu)^2}{2\sigma}\right] \quad (6)$$

where μ is the mean prime of x, and, σ is the standard deviation of x. g_a, and g_n PDFs were formed from 100 back-calculated samples, while the GSI PDF was created through three-sigma rule results for 1000 samples, all in Excel. The blue bars represent the histogram of the PDF, while the orange line represents the normal PDF curve. Based on the definition of MCS, the three parameters will be input in PLAXIS 2D through the MCS sampling from these PDF distributions.

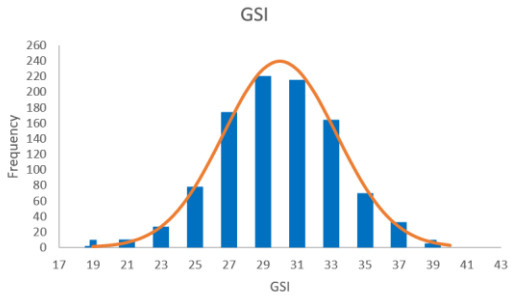

(a)

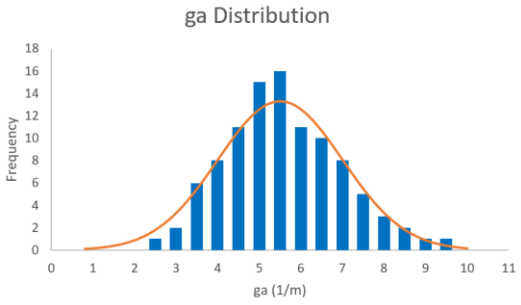

(b)

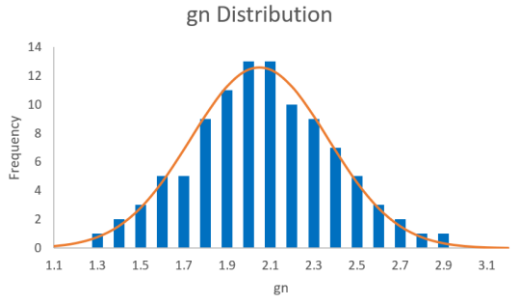

(c)

Figure 13 Hydromechanical parameter PDF distributions (a) GSI (b) g_a (c) g_n

3. Transient slope stability analysis for FOS

In PLAXIS, the strength reduction method is mainly used to calculate the safety factor, which will gradually reduce the cohesion c and friction angle φ of the material until the slope fails. The resulting strength reduction factor is the safety factor. According to the Brinkgreve et al. (2016), the strength reduction factor is expressed as:

$$\frac{c}{c_r} = \frac{\tan\varphi}{\tan\varphi_r} = \mathrm{Msf} \qquad (7)$$

where c is cohesion, c_r is the reduced cohesion, φ is the friction angle, $\varphi_r$is the reduced friction angle and, σ_n is the normal stress (Brinkgreve et al., 2016).

The designed rainfall patterns were added to the model through infiltration, and the fully-coupled transient analyses were simulated (Figure 14). The simulations were divided into four stages. The first stage was the initial steady state stage following the gravity loading configuration. After that, Phase 1 considers a no-rainfall period transient analysis of 500 hours to stabilize the GWL. The GWL level at the end of this stage is considered the pre-rainfall GWL value. Phase 2 introduces the designed rainfall event into the model, and the GWL rise is observed. The GWL at the end of this stage is considered the after-rainfall GWL value. The rise of GWL was calculated from these phases. Phase 3 calculated the FOS after a rainfall event. Figure 15 shows that the surface displacement matches the real slope conditions, where the highest displacement is found at the top of the sliding surface.

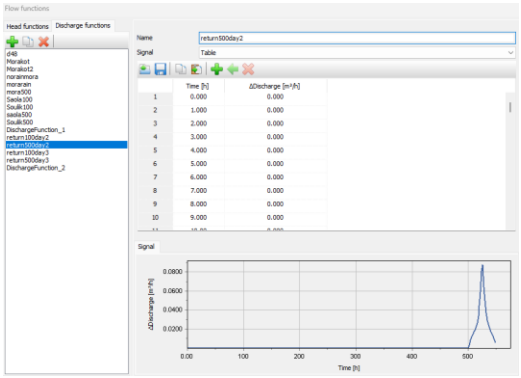

(a)

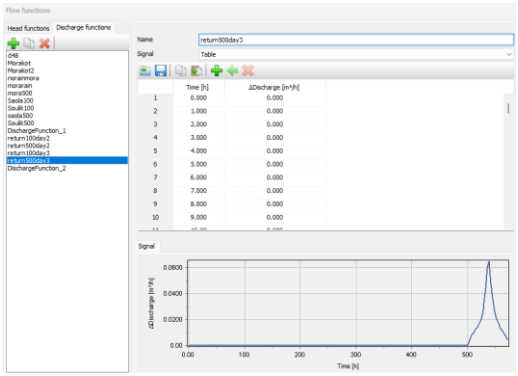

(b)

Figure 14 Input rainfall designs in PLAXIS 2D (a) 500-year 2-day (b) 500-year 3-day

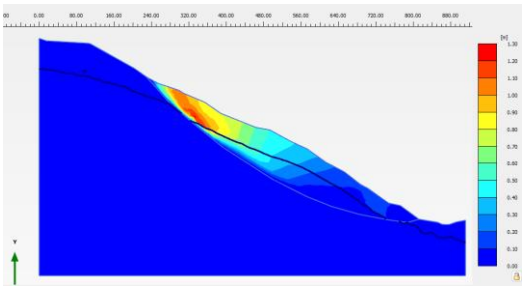

Figure 15 Surface displacement under 48-hour rainfall

4. Slope failure probability under different return intervals and rainfall durations

The Monte Carlo sampling method generates different parameter combinations for FOS calculations. A total of 4000 simulations were done, with 1000 each for the four rainfall designs. The probability of failure (P_f) for the four rainfall designs is calculated using the following equation and tabulated in Table 3. This approach can serve as a reference for risk assessment and early warning systems of large-scale landslides.

$$P_f = Pr[FOS<1] \quad (8)$$

The probability density distributions are shown in Figure 16. It is observed from the results, that the probability of failure is more for 3-day than 2-day durations. This explains that longer durations of rainfall have more damaging effect than short durations in case for deep-seated landslides. Also, it was observed that the return period didn't affect the failure probability as significantly as the durations of rainfall.

Table 3 Failure probabilities

Rainfall design (Duration (days) – Return interval (years))	Probability of failure (%)
2– 100	22
2– 500	27.4
3– 100	30.2
3– 500	35

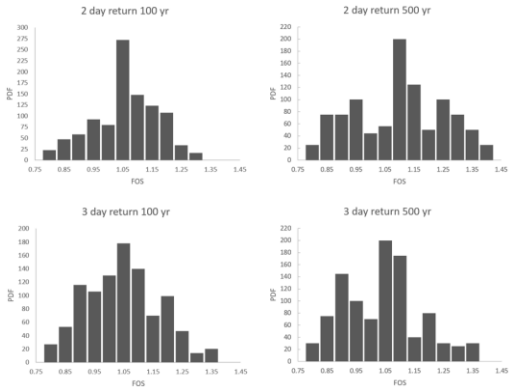

Figure 16 Probability density distribution of FOS for the 4 rainfall designs

Conclusion

This study uses FEM software for slope stability analyses and accounts for uncertainty in GSI and unsaturated VG parameters to provide a reliable probabilistic analysis for reference.

1) The GWL changes observed in the simulations were consistent with the

borehole monitored data; therefore, this model is effective for subsequent use.

2) It was observed from the results that rainfall duration is more influential than return interval on the probability of failure.
3) The probability of failure of the Lushan slope with rainfall duration of 2 days and return intervals of 100 and 500 years ranges from 22 to 27 %.
4) The probability of failure of the Lushan slope with rainfall duration of 3 days and return intervals of 100 and 500 years ranges from 30 to 35 %.

References

1. Benesty, J., Chen, J., Huang, Y., & Cohen, I. (2009). Pearson correlation coefficient. In *Noise reduction in speech processing* (pp. 1-4). Berlin, Heidelberg: Springer Berlin Heidelberg.
2. Bureau of Water Resources (2001) Handbook for Hydrological Design.
3. Brinkgreve, R.B.J., Kumaeswamy, S. and Swolfs, W.M. (2016) PLAXIS 2016 User's Manual. PLAXIS.
4. Cai, M., Kaiser, P. K., Tasaka, Y., & Minami, M. (2007). Determination of residual strength parameters of jointed rock masses using the GSI system. *International Journal of Rock Mechanics and Mining Sciences*, *44*(2), 247-265.
5. Central Geological Survey (2012). Mechanism investigation and activity observation of large-scale landslide.
6. Chang, K. T., & Huang, H. C. (2015). Three-dimensional analysis of a deep-seated landslide in central Taiwan. *Environmental Earth Sciences*, *74*, 1379-1390.
7. Chow, V. T., Maidment, D. R., & Mays, L. W. (1988). *Applied hydrology*. McGraw-Hill.
8. Chowdhury, R., Bhattacharya, G., & Metya, S. (2023). *Geotechnical slope analysis*. Crc Press.
9. Duncan, J. M. (2000). Factors of safety and reliability in geotechnical engineering. *Journal of geotechnical and geoenvironmental engineering*, *126*(4), 307-316.
10. GEO-SLOPE International Ltd. (2012). Stability modeling with SLOPE/W. An Engineering Methodology: July 2012 Edition, p.238.
11. Hammah, RE, Yacoub, TE, & Curran, JH (2009). Probabilistic slope analysis with the finite element method. In 43rd US Rock Mechanics Symposium & 4th US-Canada Rock Mechanics Symposium. OnePetro.
12. Harr, M. E. (1987). Reliability-based design in civil engineering, McGraw-Hill, New York, N.Y.
13. Johari, A., & Talebi, A. (2019). Stochastic analysis of rainfall-induced slope instability and steady-state seepage flow using random finite-element method. International Journal of Geomechanics, 19(8), 04019085.
14. Malkawi, AIH, Hassan, WF, & Abdulla, FA (2000). Uncertainty and reliability analysis applied to slope stability. Structural safety, 22(2), 161-187.
15. Morgenstern, NR, (1997). Toward landslide risk assessment in practice. In: Cruden and Fell (eds.) Landslide risk assessment, 15-24, Balkema, Rotterdam.
16. Van Genuchten, M. T. (1980). A closed-form equation for predicting the hydraulic conductivity of unsaturated soils. *Soil science society of America journal*, *44*(5), 892-898.
17. Wang, L., Tang, L., Wang, Z., Liu, H., & Zhang, W. (2020). Probabilistic characterization of the soil-water retention curve and hydraulic conductivity and its application to slope reliability analysis. Computers and Geotechnics, 121, 103460.

18. Yang, B., Yin, K., Lacasse, S., & Liu, Z. (2019). Time series analysis and long short-term memory neural network to predict landslide displacement. *Landslides*, *16*, 677-694.

---

114 年 12 月 16 日收稿

114 年 12 月 23 日修改

114 年 12 月 24 日接受